

Archana Beher, Raeesha Rahman, Iadalin Rynthiang,
Yuvashree Chandrasekaran, Sridevi Kaliaperumal,
Mukesh Kumar Dharmalingam Jothinathan*

Department of Biochemistry, Saveetha Medical College and
Hospital, Saveetha Institute of Medical and Technical Sciences
(SIMATS), Saveetha University, Chennai, Tamil Nadu, India.

Scientific paper

ISSN 0351-9465, E-ISSN 2466-2585

<https://doi.org/10.62638/ZasMat1324>



Zastita Materijala 67 ()
(2026)

Biogenic synthesis of zinc oxide nanoparticles by *Coleus amboinicus* extract: Its spectral analysis and biological activities

ABSTRACT

Zinc oxide nanoparticles (ZnONPs) were synthesized using *Coleus amboinicus* leaf extract (CALE) via a green synthesis approach. UV-Vis spectroscopy confirmed ZnONPs formation, showing a broad peak at 335 nm. FTIR analysis identified phytochemicals involved in the formation and capping of ZnO NPs, enhancing stability. SEM imaging revealed irregular shaped ZnO NPs with size ranging in 20 nm -50 nm, and EDAX confirmed the elemental compositions. ZnO NPs synthesized using CALE exhibited potent antioxidant activity in DPPH, H₂O₂, FRAP, ABTS, and NO assays. The high activity, dose-dependent inhibition, and synergistic effects of ZnO NPs and phytochemicals highlight their potential for use in biomedical and cosmetic applications to mitigate oxidative stress and inflammation. ZnO NPs synthesized from *C. amboinicus* exhibited minimal cytotoxicity at 20 µg/mL concentrations in brine shrimp. In osteosarcoma cells, ZnO NPs exerted a dose-dependent cytotoxic effect with an IC₅₀ of 89.98 µg/mL. Morphological changes and apoptosis of osteosarcoma cells confirm ZnO NPs potential as an anticancer agent.

Keywords: Zinc oxide; nanoparticles; antioxidant activity; toxicology study; anticancer activity.

1. INTRODUCTION

Nanotechnology and biotechnology are two distinct but linked fields of study that strive to improve people's quality of life by improving the materials' optical, electrical, magnetic, and catalytic properties. This is accomplished by reducing the size of the bulk materials to nano regime. As a result of the convergence of nanotechnology and biotechnology, particularly nanoscale biofabrication, a new category of materials has been developed that has the potential to be utilized in a wide variety of research disciplines [1]. Because of their unique properties and high surface area-to-volume ratio, nanoparticles (NPs), which may be prepared in a variety of different methods, are really fascinating. They are effective methods for preventing the growth of germs and reducing pollution [2] due to the properties that they possess. Plants and bacteria are examples of living organisms that can produce NPs.

The metal ions in a metal salt solution is reduced through the process of plant-mediated synthesis by making use of natural reducing agents that are found in plant extracts. After then, atoms congregate into smaller clusters, which eventually develop into NPs over the course of time [3]. Zinc oxide NPs (ZnO NPs), gained the attention of researchers due to its remarkable ability to eliminate microorganisms [4]. The researchers believe that these particles might have applications in the fields of agriculture and medicine. As a result of its unique properties, such as being antibacterial, antioxidant, photocatalytic, and photooxidation active, ZnONPs are known to be safe for human usage and are utilized in a wide variety of applications. Despite their diminutive size, they possess a distinctive band gap and a high excitonic binding energy, both of which contribute to their increased utility. Because of these characteristics, ZnONPs are currently a subject of interest in the field of research. This is especially true due to the fact that they are capable of combating a large number of harmful bacteria [5,6].

Coleus amboinicus leaves, often known as Indian borealis, is a medicinal plant with a delicate fleshy perennial that contains different phytochemicals, such as patchoulane, flavonoids, monoterpenoid (carvacrol), and bicyclic sesquiterpene (caryophyllene), and has several medical uses. It is

*Corresponding author: Mukesh Kumar
Dharmalingam Jothinathan

E-mail: itsmemukesh@gmail.com

Paper received: 18. 12. 2025.

Paper corrected: 24. 12. 2025.

Paper accepted: 07. 01. 2026.

used to treat fever, renal, hepatopathy, cough, asthma, bronchitis, cough, colic, convulsions, and vesical calculi. Metals (silver, gold NPs, etc.) and metal oxide NPs (copper oxide, cadmium oxide, etc.) were synthesized using *C. amboinicus* extract as reducing agent [7–12]. Antioxidants are extremely important for protecting cells and biological macromolecules against degenerative processes caused by free radicals and reactive oxygen species [13]. Recent investigations have demonstrated that inorganic NPs prepared through green synthesis successfully scavenge oxygen-based free radicals [14]. The biosynthesized ZnO NPs demonstrated considerable antioxidant activity. Higher ZnONPs concentrations boosted the free radical scavenging activity [15].

Fundamental toxicological evaluation states that the dosage determines whether a chemical contains high toxicity or not [16]. Brine shrimp lethality test is a useful approach for detecting cytotoxic chemicals. This approach is frequently used for pre-screening active chemicals because it is inexpensive, quick, simple, and dependable [17]. A study found that using silver NPs in commercial formulations at concentrations exceeding 12 nM might induce significant DNA damage in brine shrimp due to toxicological effects [18]. A study shows that ZnO NPs suspensions were less harmful to brine shrimp than their metallic counterparts under similar conditions. Further, the findings indicated that ZnO NPs exhibit considerable anticancer activity *in vitro* [19]. ZnO NPs demonstrated *in vitro* anticancer activity

against the HeLa cell line, with an IC₅₀ value of 38.60 µg/mL, compared with the reference standard cisplatin. This study revealed that ZnO NPs from shilajit extract have a strong cytotoxic impact on human cervical cancer cell types [20].

In the present study, ZnO NPs were prepared using green synthesis route with *C. amboinicus* extract. The prepared ZnO NPs were characterized using UV-Vis and Fourier transform infrared (FTIR) spectroscopy where UV-Vis spectrophotometry was used to investigate the absorption spectrum of the reaction suspension containing the synthesized ZnO NPs and the functional characteristics of the NPs were determined by FTIR spectrum. Morphologies, elemental contents, and particle sizes were studied using SEM equipped with an EDAX. Antioxidant activity of ZnO NPs is elucidated through DPPH, H₂O₂, FRAP, ABTS, and NO assays. Cytotoxicity activity of ZnO NPs is determined using brine shrimp model. Further, MTT assay was conducted to analyse the anticancer activity against osteosarcoma cells.

2. MATERIALS AND METHODS

2.1. Synthesis of ZnO NPs

ZnO NPs are synthesized using CALE and characterized using various techniques [21]. Figure 1 displays the schematic illustration for the green synthesis of ZnO NPs. *C. amboinicus* leaves were collected from Chennai, Tamilnadu, India.

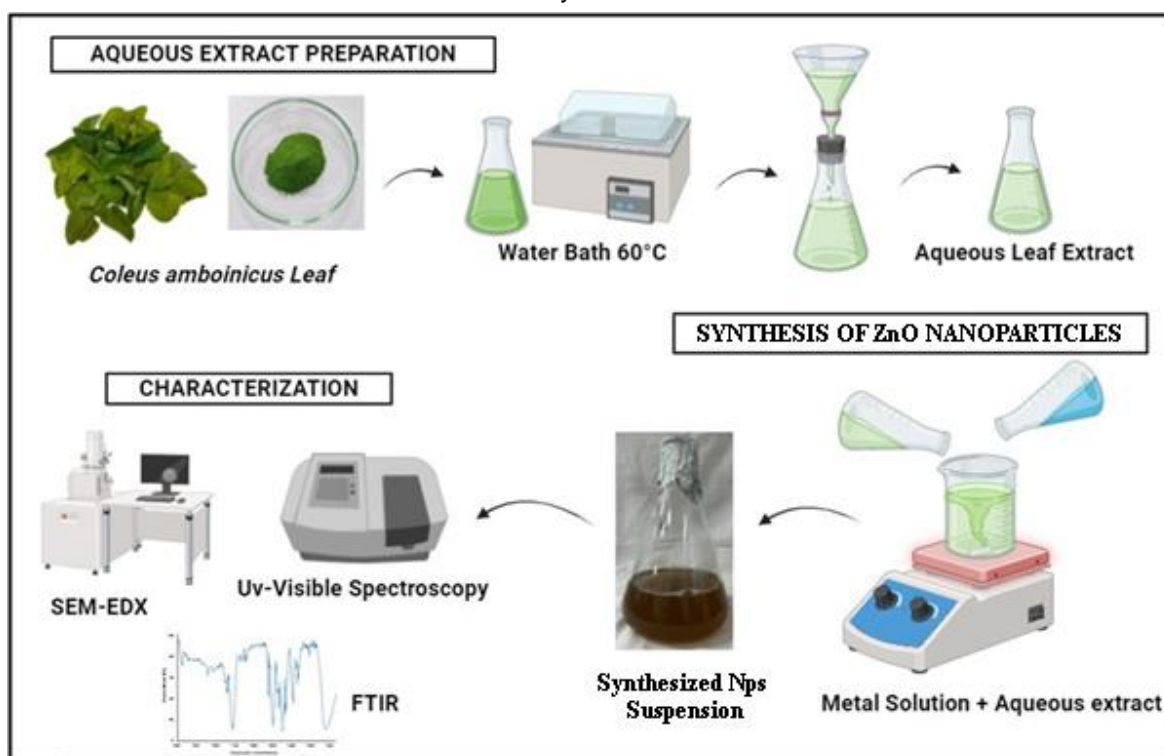


Figure 1. Graphical abstract of Zinc nanoparticle synthesis and its characterization.

The samples were verified by the Center for Advanced Studies in Botany, University of Madras, Chennai, India. *C. amboinicus* leaves were chopped into small pieces, washed 3 times with distilled water, and air-dried in a shaded area for three days. Once the *C. amboinicus* leaves had fully dried, they were ground into a fine powder and stored for future use. Subsequently, 25 g of *C. amboinicus* leaf powder was transferred into a 300 mL of double-distilled H₂O at 60°C for 20 min. Afterwards, the extract was filtered using a muslin cloth and further refined using Whatman filter paper with a diameter of 125 mm. The filtered solution was stored at 4° C for further use.

A 5mM zinc nitrate (Zn (NO₃)₂) solution was prepared by dissolving it in 300 mL of distilled water. To synthesize ZnO NPs, 10 mL of CALE was combined with 90 mL of a ZnCl₂ solution (5 mM) and agitated at 35°C. The acidity of the reaction mixture was consistently checked and recorded. Subsequently, the reaction mixtures were incubated in a dark room on a rotating shaker at 40°C and 300 rpm for 3 h. Visual evaluation of the reaction mixture color was followed by incubation at room temperature for 72 h. After the incubation period, a total color change was detected in the reaction mixture, indicating the successful synthesis of the NPs. Conversely, the control containing only Zn (NO₃)₂ exhibited no color change.

2.2. Characterization of ZnO NPs

The ZnO NPs were characterized using UV- vis spectroscopy, FTIR spectroscopy, and SEM with EDAX. Synthesized ZnO NPs was first detected using UV-visible spectrophotometry in the 200-800 nm range. The FTIR analysis, at 4000-400 cm⁻¹, successfully identified the specific functional groups present on the ZnO NPs. Morphology and material confirmation were evaluated using SEM and EDAX.

2.3. Antioxidant activity

2.3.1. DPPH radical scavenging assay

A 2,2-diphenyl-1-picrylhydrazyl (DPPH) radical scavenging assay was performed based on the literature procedure [22]. Different concentrations (10 µg/mL -50 µg/mL) of the CALE mediated ZnO NPs were added to 200 µL of the DPPH working solution. The plate was incubated in the dark for 10 min at room temperature. The absorbance of the samples was recorded, and the percentage of DPPH scavenging activity was calculated using the formula,

$$\% \text{Radical scavenging activity} = \frac{A_c - A_t}{A_c} \quad (1)$$

Where, A_c is the absorbance of the control and A_t is the absorbance of the test

2.3.2. Hydrogen peroxide radical scavenging assay

Hydrogen peroxide radical scavenging assay was examined based on the literature procedure [23]. A solution of the test sample (ZnO NPs) and a standard sample of ascorbic acid at varying concentrations (10 µg/mL -50 µg/mL) were individually added to 0.6 mL of H₂O₂ solution. After 10 min of incubation in the dark, the absorbance of the reaction solution was observed spectrophotometrically at 230 nm. The percentage of H₂O₂ scavenging activity was calculated using the eqn. (1).

2.3.3. FRAP assay

FRAP assay was conducted using the literature technique [24]. FRAP reagent (2.3 mL) was mixed with 0.7 mL of CALE at different concentrations (10 µg/mL -50 µg/mL). The mixture was then incubated at 37°C for 30 min in the dark. The absorbance was measured at 593 nm using a spectrophotometer.

2.3.4. ABTS

The ABTS radical cation (ABTS⁺) was examined using the procedure mentioned in the literature [24]. This reagent was stored under refrigeration conditions for at least 24 h. The reagent was diluted with 50% ethanol until an absorbance of 1.0 at 734 nm. 250 µL ABTS⁺ and 20 µL of sample (10 µg/mL -50 µg/mL dissolved in distilled water) were added. The radical scavenging activity was calculated.

2.3.5. Nitric oxide radical inhibition assay

Nitric oxide radical inhibition was estimated using the previous literature procedure [24]. The reaction mixture (3mL) was incubated at 25°C for 150 min. After incubation, 0.5mL of the reaction mixture was mixed with 1 mL of sulfanilic acid reagent (0.33 % in 20 % glacial acetic acid) and allowed to stand for 5 min for complete diazotization. Then, 1 mL of naphthyl ethylene diamine dihydrochloride was added, mixed, and allowed to stand for 30 min at 25°C. A pink chromophore is formed under diffused light. The absorbance of these solutions was measured at 540nm.

2.4. Toxicology on brine shrimp

The brine shrimp lethality assay (BSLA) was used to evaluate the cytotoxicity of ZnO NPs synthesized using CALE at different concentrations (5 µg/mL, 10 µg/mL, 20 µg/mL, 40 µg/mL, and 80 µg/mL).

2.5. Cell viability in the MTT assay

Fibroblasts were cultured individually in 96-well plates at a density of 5×10³ cells per well in

DMEM supplemented with 10% FBS and 1X antibiotic solution. The cells were then placed in a CO₂ incubator at 37°C with a CO₂ concentration of 5%. The cells were rinsed with 100 µL of 1XPBS and then exposed to ZnO NPs. Subsequently, the cells were incubated at 37°C with 5% CO₂ for 24 h. Following the treatment, the liquid in the container was removed, and the cells were exposed to MTT (0.5 mg/mL in 1XPBS) at a temperature of 37°C for 4 h. After the incubation period, the media containing MTT was removed, the cells were rinsed with 100 µL of PBS, and the crystals formed were dissolved in 100 µL of DMSO. The absorbance of the generated purple-blue formazan dye was quantified at 570 nm using a microplate reader.

To examine the impact of ZnO NPs on cell morphology, 2,00,000 normal fibroblast cells were evenly distributed in six-well plates and subjected to either ZnO NPs treatment or no treatment for 24 h. After treatment, cells were rinsed with PBS and examined using an inverted phase-contrast microscope.

3. RESULTS

3.1. UV spectrophotometer

Figure 2a shows the UV-visible spectrum of ZnO NPs synthesized using CALE, which provides

crucial insights into the optical properties and formation mechanism of the NPs. In this spectrum, a prominent peak appeared at ~335 nm is observed which is the characteristic peak for semiconductor ZnO NPs. Here, the peak position was slightly higher than the typical ZnONPs peak (~330 nm), which could imply a marginal increase in particle size or slight aggregation owing to the change in the synthesis procedure. The broad nature of the absorbance peak can also imply a range of particle sizes, indicating polydispersity. The phytochemicals present in CALE play a crucial role in reducing Zn ions to NPs, and stabilizing them, and preventing excessive growth and agglomeration. The exact mechanism involves the reduction of Zn²⁺ ions to ZnO by the bioactive compounds present in the extract, followed by capping the NPs by these biomolecules. This capping is essential because it provides stability and agglomeration and ensures that, the NPs remain dispersed in the medium. Thus, this green synthesis approach using the inherent reducing and capping agents of *C.amboinicus* provides, a renewable and environmentally friendly method of synthesizing ZnO NPs that can be used in medicine, agriculture, and environmental conservation [25].

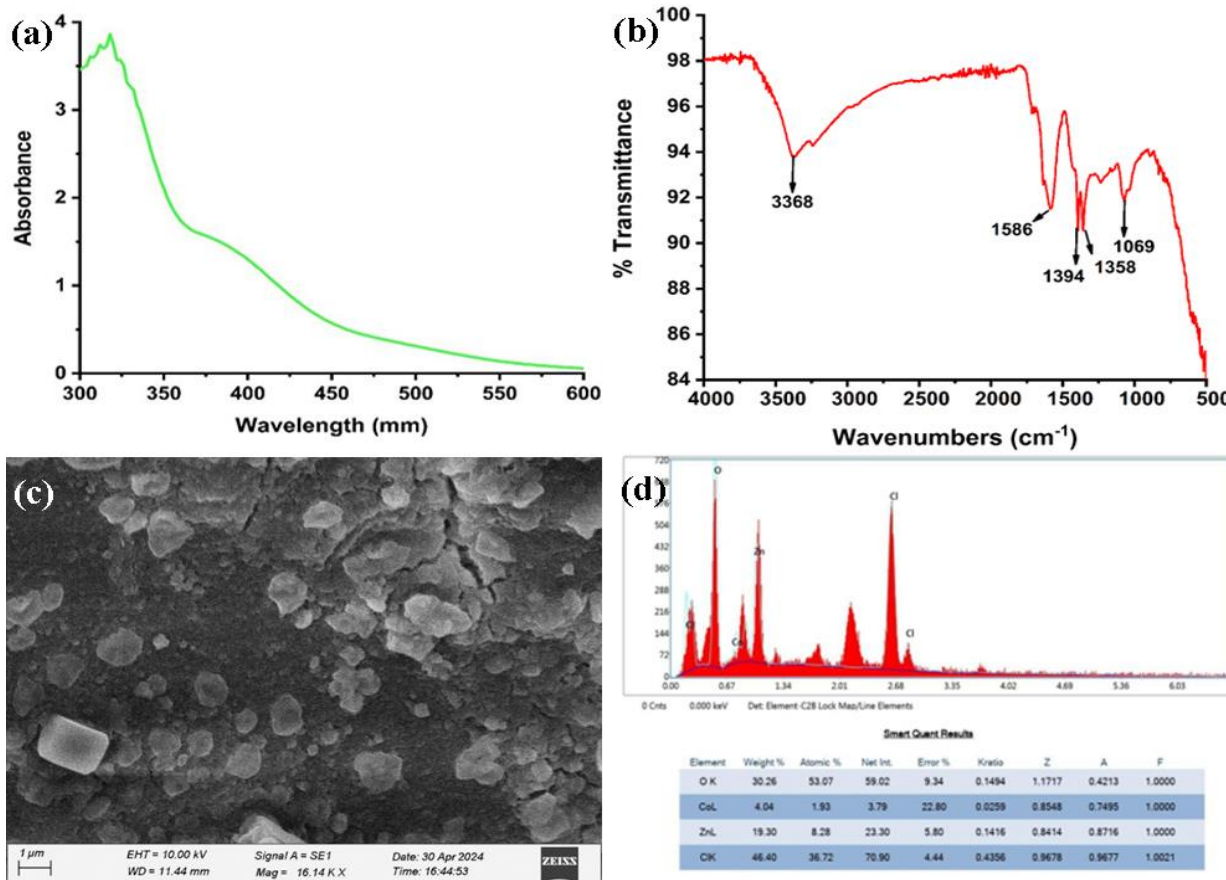


Figure 2. (a) UV-Vis spectrum, (b) FTIR, (c) SEM image, and (d) EDAX spectrum of the ZnO NPs

3.2. FTIR

The FTIR spectrum (4000-400 cm^{-1} range) of ZnO NPs synthesized from CALE revealed significant information about the functional groups present on the NPs surface and their interaction with the biomolecules in the plant extract [Figure 2b]. In the FTIR spectroscopic analysis, the responsible chemical groups (minor/major) involved in the formation and capping of ZnO NPs in the leaf extract were not masked. The FTIR spectrum of ZnO NPs show, several distinct peaks, each corresponding to specific vibrational modes of the chemical bonds present. The peaks were observed at 3368.8 cm^{-1} , 1586.2 cm^{-1} , 1394.1 cm^{-1} , 1358.7 cm^{-1} , and 1069.9 cm^{-1} , and in the 620 cm^{-1} -400 cm^{-1} range. The broad peak at 3368.8 cm^{-1} is characteristic of O-H stretching vibrations, which are commonly associated with hydroxyl groups (OH) found in alcohols and phenols. The peaks at 1586.2 cm^{-1} indicate C=C stretching vibrations of the aromatic rings, indicating the presence of aromatic compounds in the plant extract. The peak in the range of 1394.1 cm^{-1} can be attributed to the symmetric stretching vibrations of carboxylate anions (COO^-). The peak at 1358.7 cm^{-1} corresponds to the bending vibrations of C-H bonds in alkanes. The presence of this peak indicates the presence of aliphatic hydrocarbons or aliphatic chains from organic compounds in the plant extract on the surface of the ZnO NPs. The peak at 1069.9 cm^{-1} is characteristic of C-O stretching vibrations, which can be associated with alcohols, ethers, or esters. The multiple peaks observed in the 620-400 cm^{-1} range are typically associated with the stretching vibrations of Zn-O bonds and the lattice vibrations of ZnO NPs. These peaks confirm the formation of ZnO NPs, indicating that the Zn ions were successfully reduced and oxidized to form ZnO structures.

The presence of these peaks provides direct evidence of the Zn-O bonding and the crystalline nature of the ZnO NPs. These functional groups not only confirm the successful synthesis of ZnO NPs but also highlight the role of natural compounds from *C. amboinicus* in providing biocompatible and stable NPs formulations. The presence of hydroxyl groups from plant extracts or water molecules are involved in the capping and stabilization of ZnO NPs. These hydroxyl groups may be derived from phenolic compounds present in CALE, which play a significant role in stabilizing NPs. Aromatic compounds, such as flavonoids and other polyphenols, are also known to participate in the capping of NPs, providing stability through π - π interactions and other bonding mechanisms. The presence of carboxylate-containing compounds, possibly procured from organic acids in plant

extracts, interact with the surface of the ZnO NPs, providing stability, and preventing aggregation. The aliphatic groups contributed to the hydrophobic stabilization of the NPs. The alcohol and ether from plant extracts provide steric hindrance, preventing NPs from aggregating. Furthermore, the interaction of these functional groups with the NPs surface can influence the biological activity of ZnO NPs. The presence of hydroxyl, carbonyl, and other functional groups can enhance the biocompatibility and reactivity of NPs, making them suitable for various applications, including antimicrobial, antioxidant, and catalytic activities. The use of the plant extracts for green and sustainable NPs synthesis not only reduces the environmental impact associated with traditional chemical synthesis but also leverages the natural properties of plant extracts to produce NPs with enhanced functionality [26].

3.3. SEM

The SEM image of ZnO NPs synthesized from CALE is shown in Figure 2c and offers a detailed view of the NPs morphology, size distribution, and surface characteristics. The NPs exhibit a range of shapes, predominantly some irregular forms. The average particle size observed in the SEM images ranged from 20 nm to 50 nm. The size and shape of the NPs are critical parameters that influence their biological activity, solubility, and interaction with cells and tissues. Some degree of agglomeration was observed in SEM image, which is common in NPs synthesis, especially when using natural extracts. Agglomeration occurs when NPs cluster together due to van der Waals forces or hydrogen bonding. While NPs agglomeration is inevitable, the overall dispersion of the NPs indicates that the phytochemicals in the leaf extract effectively stabilize ZnO NPs and reduce excessive aggregation [26].

3.4. EDAX

The EDAX spectrum of ZnO NPs synthesized from CALE provides comprehensive elemental analysis and confirms the presence of various elements in the synthesized NPs. The EDAX spectrum of ZnO NPs in Figure 2d shows distinct peaks corresponding to zinc (Zn), oxygen (O), carbon (C), and chlorine (Cl). The presence of Zn was confirmed by the prominent peaks at around 1 and 8.6 keV, which are characteristic of Zn. This result confirms the successful synthesis of ZnO NPs because, zinc is the primary component of the NPs. The presence of O and C peaks indicates the involvement of phytochemicals from CALE in the synthesis process, likely acting as capping agents. The quantitative analysis provided in the table shows the weight and atomic percentage of each element present in the sample. For instance,

Zn constitutes around 19.30 wt.%, which is substantial and confirmed the successful synthesis of ZnO NPs. The relatively high O and C contents (30.26 wt.% and 46.40 wt.%, respectively) further support the role of plant extract components in stabilizing NPs. The quantitative analysis of these elements highlights the role of organic molecules in the capping and stabilizing NPs, thus ensuring their stability and functionality [27]. The presence of these elements indicates that organic molecules from the plant extract are adsorbed onto the NPs surface, providing stability and preventing agglomeration.

3.5. Antioxidant Activity

3.5.1. DPPH Assay

The ability of ZnO NPs to scavenge DPPH free radicals was measured using a DPPH assay in which doses of 10 µg/mL -50 µg/mL. The efficiency of ZnO NPs was determined in comparison with standard (ascorbic acid) based on their ability to reduce DPPH radicals. An increase in the ZnO NPs concentration provided better radical

scavenging activity in terms of inhibiting the formation of DPPH radicals. This indicates that the presence of bioactive chemicals in the extract influences this process. The scavenging capacity of ZnO NPs (10 µg/mL -50 µg/mL) against DPPH was determined, and the values were noted. The free radical scavenging trait of ZnO NPs synthesized from CALE was executed using a standard assay protocol, and the acquired data are illustrated in Figure 3a. The report provided that with an increase in ZnO NPs concentrations, an impressive increase in antiradical activity was achieved in the test. The bar graph shows the percentage inhibition of DPPH radicals at various concentrations for both standard and ZnO NPs. At all tested concentrations, ZnO NPs exhibited substantial DPPH radical scavenging activity comparable to the standard. The percentage of inhibition increases with concentration, indicating a dose-dependent antioxidant effect. At the highest concentration (50 µg/mL), ZnO NPs exhibited approximately 80% inhibition, which is close to the inhibition exhibited by the standard.

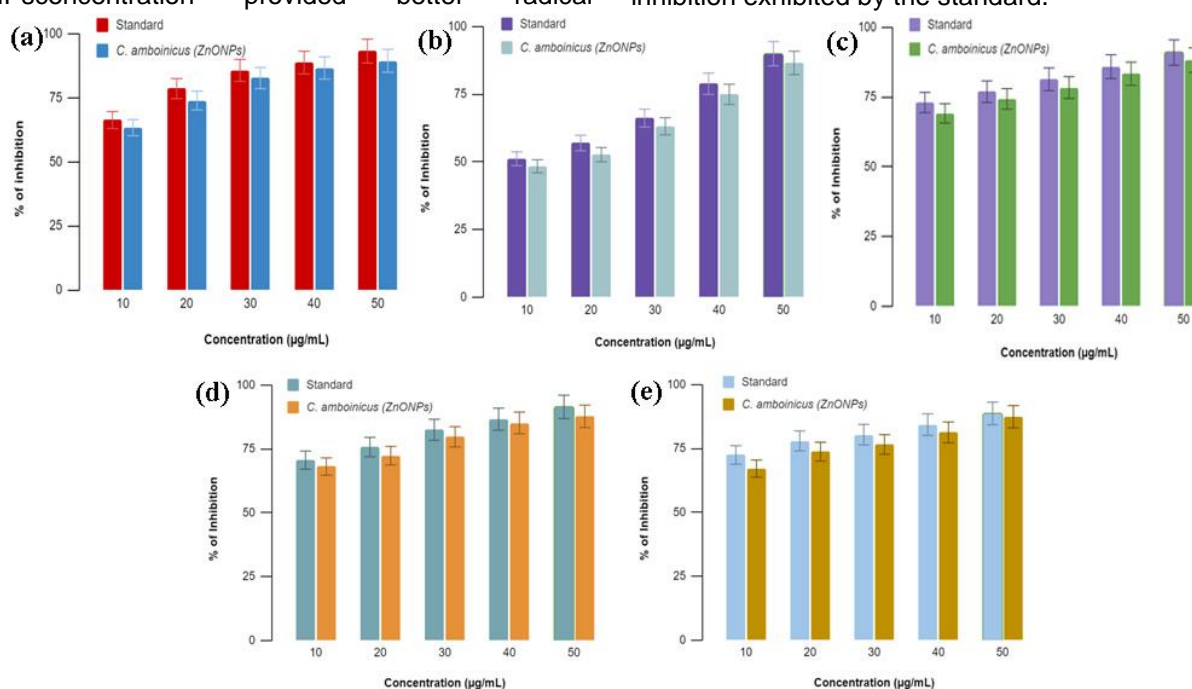


Figure 3. (a) DPPH assay, (b) H₂O₂ assay, (c) ferric-reducing antioxidant power assay, (d) ABTS assay, and (e) nitric oxide assay of the ZnO NPs

3.5.2. Hydrogen peroxide assay

Hydrogen peroxide is relatively stable but can generate highly reactive hydroxyl radicals through Fenton reactions, contributing to oxidative stress. The H₂O₂ assay evaluates the ability of a compound to scavenge hydrogen peroxide. The inhibitory effects on hydroxyl radicals by the formed ZnO NPs were perceived varying amounts, and the

results are presented in Figure 3b. Vitamin C was used as the comparative reference standard. The graphical data for the H₂O₂ assay of ZnO NPs synthesized from CALE reveal their effective hydrogen peroxide scavenging activity. The bar graph depicts the percentage of H₂O₂ inhibition at different concentrations (10 µg/mL -50 µg/mL) for both standard and ZnO NPs. At all tested concentrations, the ZnO NPs exhibited notable

H₂O₂ scavenging activity, which increased with concentration. At the highest concentration (50 µg/mL), ZnO NPs achieved nearly 80% inhibition, closely matching the activity of the standard. These results indicate that ZnO NPs can effectively neutralize hydrogen peroxide, potentially reducing oxidative damage.

3.5.3. Ferric-reducing antioxidant power assay

Figure 3c, graphical data for the FRAP assay of ZnO NPs synthesized from CALE illustrates the significant ferric-reducing anti-oxidant power. The graph shows the percentage reduction at various concentrations (10 µg/mL - 50 µg/mL) for both the standard (ascorbic acid) and the ZnO NPs. At all tested concentrations, ZnO NPs exhibit strong reducing power comparable to that of the standard. The percentage reduction increased with concentration, indicating a dose-dependent antioxidant effect. At the highest concentration (50 µg/mL), ZnO NPs reduced by nearly 90%, which is similar to the reduction exhibited by the standard.

3.5.4. ABTS Assay

The graphical data for the ABTS assay of ZnO NPs synthesized from CALE indicated their significant antioxidant activity. The bar graph [Figure 3d] presents the percentage of ABTS radical cation inhibition at various concentrations (10 µg/mL - 50 µg/mL) for both standard and ZnO NPs. At all tested concentrations, ZnO NPs exhibited notable ABTS radical scavenging activity, which increased with concentration. At the highest ZnO NPs concentration (50 µg/mL), nearly 90% inhibition was achieved, closely matching the activity of the standard. This result indicates that ZnO NPs can effectively neutralize ABTS radicals and exhibit potent antioxidant activity. Chemically provoked ABTS free radicals for scavenging is a specific and highly sensitive test. Our results concur with currently available reports.

3.5.5. Nitric oxide assay

The NO assay evaluates the ability of a compound to scavenge nitric oxide, a reactive nitrogen species that plays a significant role in various pathological and physiological activities. The graphical data for the NO assay of ZnO NPs shown in Figure 3e illustrate the effective nitric oxide scavenging activity. The bar graph depicts the percentage of NO inhibition at different concentrations (10-50 µg/mL) for both standard and ZnO NPs. At all tested concentrations, ZnO NPs exhibited substantial NO scavenging activity, which increased with concentration. At the highest concentration (50 µg/mL), ZnO NPs exhibited nearly 80% inhibition, similar to the activity of the standard. The biogenically formed ZnO NPs directly competed with oxygen and inhibited the

concentration of reactive radical species, thereby bearing a trait of counteracting deleterious nitric oxide formation. Thus, it was concluded that they may possess activity to hinder the ill effects of *in vivo*-generated nitric oxide.

The high anti-oxidant activity of ZnO NPs can be attributed to the bioactive compounds present in CALE. These phytochemicals, including flavonoids, phenolic acids and terpenoids, possess strong reducing properties. During the synthesis of ZnO NPs, these compounds not only form NPs but also cap and stabilize the NPs, enhancing their antioxidant capabilities. The nanoscale size of ZnO NPs also contributes to their high anti-oxidant activity. The large surface-area-to-volume ratio of the NPs allows for more efficient electron-transfer reactions, improving overall antioxidant activity of ZnO NPs.

3.6. Brine shrimp lethality assay for ZnO NPs

The BSLA graph in Figure 4a presents valuable data on the cytotoxicity of ZnO NPs synthesized from *C. amboinicus*. This assay, which is commonly used to evaluate substances toxicity, measures the survival rate of brine shrimp nauplii over a given period. The x-axis of the graph indicates the concentration of ZnO NPs in µg/mL, ranging from 5 µg/mL to 80 µg/mL, including the control group with no NPs. The y-axis reflects the percentage of live nauplii, indicating the survival rate at Day 1 and Day 2. The control group, which served as the baseline, had a high percentage of live nauplii (close to 100%) on both days. The high survival rate indicates that in the absence of ZnO NPs, brine shrimp do not experience significant mortality, establishing a benchmark for assessing the impact of NPs.

At the lowest concentrations tested (5 µg/mL, 10 µg/mL, and 20 µg/mL), the survival rate of nauplii remained high and comparable to that of the control group. On Day 1, the survival rate was nearly 100%, and by Day 2, there was a slight decrease, but it remained very close to the initial %. This indicates that at these low concentrations, ZnO NPs exhibit minimal cytotoxic effects. However, as the concentration increased further to 40 µg/mL and 80 µg/mL, a noticeable decline in the survival rate of nauplii was observed. At 40 µg/mL, the survival rate on day 1 was slightly lower than that at the lower concentrations, and by Day 2, there was further reduction, indicating moderate cytotoxicity. At 80 µg/mL, the decrease in the survival rate was more pronounced on day 1, and further declined by day 2. This significant reduction at the highest ZnO NPs concentration indicates a higher level of cytotoxicity, indicating that ZnO NPs become increasingly toxic as their concentration increases. The time-dependent effect of the NPs is

also evident in the graph. Across all concentrations, including the control, there was a slight decline in the survival rate from Day 1 to Day 2. This decline could indicate a natural decrease in brine shrimp viability over time or a cumulative effect of NPs exposure. The slight decrease observed in the control group indicates that some of the decline could be attributed to natural factors, whereas the more significant decreases at higher concentrations likely reflect the toxic impact of the NPs.

From the data presented in the BSLA graph, several conclusions can be drawn. First, ZnO NPs synthesized from *C. amboinicus* start to show cytotoxic effects at concentrations beyond 20 $\mu\text{g/mL}$, with noticeable effects at 40 $\mu\text{g/mL}$ and 80 $\mu\text{g/mL}$. This indicates a threshold concentration at which NPs become harmful to brine shrimp. Second, the time-dependent decline in survival indicates the presence of cumulative toxic effects or that prolonged exposure to NPs intensifies their cytotoxicity. Lastly, concentrations of ZnO NPs at or below 20 $\mu\text{g/mL}$ appear to be relatively safe for brine shrimp because, they exhibit minimal cytotoxic effects, indicating a potential safe range for these NPs. This information can be used to develop conditions and precautions for the

appropriate use and disposal of ZnO NPs so that they can be of benefit without negatively affecting the environment. These findings highlight the importance of careful consideration of NPs concentration and exposure duration in their applications, as well as the need for further research to fully understand their toxicological profiles and mechanisms of action [28].

BSLA is a simple, rapid and cost-effective bioassay widely used for preliminary toxicity screening of nanomaterials, chemicals and natural products. In this assay, *Artemia salina* nauplii serve as a sensitive biological model to assess general cytotoxicity and dose-dependent toxic responses. Hatched nauplii were exposed to different concentrations of ZnO NPs, and mortality was monitored over 24 and 48 hr. The percentage survival was calculated based on the number of live nauplii relative to the initial count. This model is considered a reliable indicator of acute toxicity and provides an initial assessment of the potential biological and environmental safety of synthesized NPs before advancing to higher-order *in vitro* or *in vivo* studies. Previous studies have demonstrated a good correlation between BSLA toxicity outcomes and cytotoxic effects observed in mammalian cell systems, making it a useful first-line screening tool.

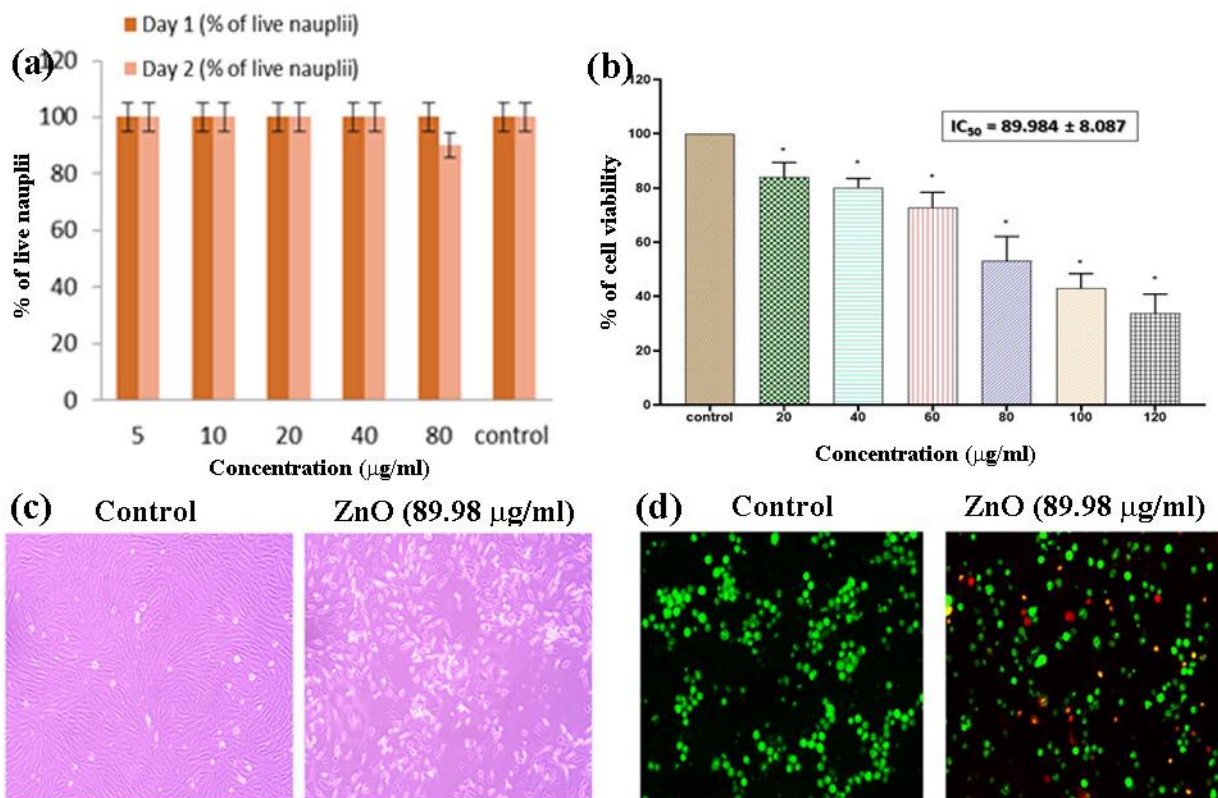


Figure 4. (a) Brine shrimp lethality assay, (b) MTT assay, (c) effect of ZnO NPs on the morphology of human osteosarcoma cells (MG-63), and (d) detection of apoptotic cells in ZnO NPs treated osteosarcoma cells by AO/EtBr dual staining

3.7. MTT Assay

The cytotoxic effects of ZnO NPs on osteosarcoma cells are shown in Figure 4b. Cells were exposed to ZnO NPs (20 µg/ml – 120 µg/ml) for 24 h, and cell viability was assessed using the MTT assay. The x-axis indicates the concentration of ZnO NPs in µg/mL, while the y-axis shows the percentage of cell viability compared to the control (untreated cells). Data are presented as mean ± SD ($n = 3$). * Denotes statistical significance ($p < 0.05$) between the control and drug treatment groups. It was observed that the control group exhibited near 100% viability, indicating normal cell growth in the absence of ZnO NPs. A dose-dependent decrease in cell viability was observed as the concentration of ZnO NPs increased from 20 µg/ml-120 µg/ml. The IC₅₀ value was approximately 89.98 µg/ml, indicating that this concentration is required to reduce the viability of osteosarcoma cells by 50%. ZnO NP exhibits cytotoxic effects on osteosarcoma cells, with increased concentration leading to higher cell death. This indicates that ZnO NPs could effectively act as an anti-cancer agent against osteosarcoma cells.

Figure 4c illustrates the effect of ZnO NP on cell morphology of human osteosarcoma cells (MG-63). Cells were incubated with ZnO NPs (89.98 µg/ml) for 24 h and observed under an inverted phase-contrast microscope. There was a reduction in the number of cells, cell shrinkage, and cytoplasmic membrane blebbing after ZnO NPs treatment. It has been observed that control cells exhibit a typical elongated, fibroblast-like morphology. Treated cells display significant morphological changes, appearing more rounded and detached, which are typical features of apoptosis and cell death. These morphological changes indicate that ZnO NPs induces apoptosis and other forms of cell death in osteosarcoma cells. The change from elongated to rounded shapes indicates loss of cell adhesion, a hallmark of apoptosis [29].

Detection of apoptotic cells in ZnO NPs (89.98 µg/ml) treated osteosarcoma cells by AO/EtBr dual staining. Human osteosarcoma cells were treated with ZnO NPs for 24 h. After treatment, cells were incubated with AO/EtBr dual staining. An inverted fluorescence microscope was used for capturing images. Control cells displayed a consistent green color, whereas cells treated with ZnO NPs displayed yellow, orange, and red signals, as shown in Figure 4d. Staining confirms that ZnO NPs treatment leads to cell death, primarily via apoptosis. The presence of red and orange cells correlated with morphological changes and decreased viability observed in the MTT assay and morphological analysis. Collectively, these findings indicate that ZnO NPs from

C. amboinicus is effective in inducing cytotoxicity and apoptosis in human osteosarcoma cells, providing potential for further investigation as a therapeutic agent. Each analysis provides a detailed view of the cellular response to ZnONPs, which is aligned with the potential anti-cancer properties highlighted in this preliminary research [29].

4. DISCUSSION

UV-Vis spectroscopy distinguished the SPR peak of ZnO NPs at 335 nm and a slight red shift hinting at size differences, signifying effective dispersion similar to the work done by Janani et al. [25]. The FTIR spectral bands indicate the functional groups present in the plant extract, which includes the -OH and -COO- groups responsible for the formation and capping of the NPs. In comparison to Ramesh et al. [30], ZnO NPs have a better distributive profile and stabilization, showing marked cytotoxicity and boosting antioxidant properties. Morphological analysis using SEM revealed moderate dispersion and heterogeneous form and dimensions, whereas EDAX analysis of the nanostructures revealed that they contained Zn, O, C, and Cl, where phytochemicals were evident to provide good stabilization. The antioxidant potential of ZnO NPs was determined using DPPH, H₂O₂, FRAP, ABTS, and NO assays, which indicated higher antioxidant activity than ZnO NPs synthesized from *Acacia nilotica* and *Cnidioscolusa conitifolius* [25,29]. This high activity is due to the phytochemicals in the leaf extract and the elevated surface-area-to-volume ratio of the nanoparticles; therefore, it could be recommended for use in health supplements, pharmaceuticals, and skin products. In this study, cytotoxicity tests were conducted using BSLA to ascertain the safety of ZnO NPs at concentrations up to 20 µg/mL, whereas toxicity was increased at 40 and 80 µg/mL, indicating the need for better precautions while using ZnO NPs, especially in aquatic systems. ZnO NPs from *Tinospora cordifolia* showed a broader cytotoxic effect, the present study has observed considerable extent of apoptosis in osteosarcoma cells using ZnO NPs from *C. amboinicus* [31,32]; however, this points toward the therapeutic potential of such forms of NPs but also the risks involved in their utilization and subsequent disposal.

The MTT assay and morphological studies conducted on osteosarcoma cells showed that ZnONPs, have notable cytotoxicity with an IC₅₀ of nearly 89.98 µg/mL. Using AO/EtBr dual staining, it was observed that ZnO NPs could induce apoptosis in osteosarcoma cells, which explains its toughening impact as an anti-cancer drug [33]. Overall, ZnO NPs prepared from *C. amboinicus* possess strong antioxidant activity and promising anticancer effects. At higher concentrations, they

are toxic to cells; therefore, their use and disposal must be well considered.

5. CONCLUSION

The green synthesis of ZnO NPs using CALE exhibited strong antioxidant and promising anticancer properties. UV-visible spectroscopy, FTIR, spectroscopy, and SEM with EDAX confirmed effective dispersion, functional group involvement, and ZnO NPs stabilization. The NPs exhibited significant antioxidants in DPPH, H₂O₂, FRAP, ABTS, and NO assays. Cytotoxicity studies revealed that ZnO NPs are safe at concentrations up to 20 µg/mL in brine shrimp, showing heightened toxicity at 40 and 80 µg/mL. Additionally, the MTT assay demonstrated their potential to induce apoptosis in osteosarcoma cells, with an IC₅₀ of around 89.98 µg/mL. While ZnO NPs hold potential in healthcare, pharmaceutical, and cosmetic applications, caution is needed regarding their use and disposal because of their high toxicity at high concentrations. Future studies will focus on optimizing their safe application to harness their benefits while minimizing environmental and health risks.

Declaration of interest

The authors declare that they have no known competing financial interests or personal relationships that could have appeared to influence the work reported in this paper.

Funding

This research did not receive any specific grant from any funding agency in the public, commercial or not-for-profit sector.

Author contribution statement

6. REFERENCES

- [1] Y.Hou, Y.Ren, Y.Shi, X.Jin, Y.Dong, H.C. Zhang (2020) *C. aromaticus* leaf extract mediated synthesis of zinc oxide nanoparticles and their antimicrobial activity towards clinically multidrug-resistant bacteria isolated from pneumonia patients in nursing care. *Mater Res Express.*; 7(9): 95015. doi 10.1088/2053-1591/abb427
- [2] M.Pezzoni, P.N.Catalano, R.A.Pizarro, M.F. Desimone, G.J.A. Soler-Illia, M.Bellino, et al. (2017) Antibiofilm effect of supramolecularly templated mesoporous silica coatings. *Mater Sci Eng C*; 77, 1044–9. <https://doi.org/10.1016/j.msec.2017.04.022>
- [3] A.Behera, M.K.D.Jothinathan (2025) Biogenic Nanoparticles of Co, Zn, Se and Ni via *Shorea robusta* Extract: Comparative Insights into Antimicrobial, Antioxidant and Toxic Effects. *Nano LIFE*, 2550011. <https://doi.org/10.1142/S1793984425500114>
- [4] M. T. Ansari, F. Sami, F. A. Khairudin, M. Z. Atan, T. A. bin Tengku Mohamad, S.Majeed, et al. (2018) Applications of zinc nanoparticles in medical and healthcare fields. *Curr Nanomed (Formerly: Recent Patents on Nanomedicine)*, 8(3), 225-233. <https://doi.org/10.2174/2405461503666180709100110>
- [5] S.K.Chaudhuri, L.Malodia (2017) Biosynthesis of zinc oxide nanoparticles using leaf extract of *Calotropis gigantea*: characterization and its evaluation on tree seedling growth in nursery stage. *Appl Nanosci.* 7(8):501–12. <https://doi.org/10.1007/s13204-017-0586-7>
- [6] E. Gurgur, S. S. Oluyamo, A. O. Adetuyi, O. I. Omotunde, A. E. Okoronkwo (2020) Green synthesis of zinc oxide nanoparticles and zinc oxide–silver, zinc oxide–copper nanocomposites using *Bridelia ferruginea* as biotemplate. *SN Appl Sci*, 2(5), 911. <https://doi.org/10.1007/s42452-020-2269-3>
- [7] A. Behera, N. Ranjith, S. Balasubramani, I. Rynthiang, M. K. Dharmalingam Jothinathan (2025) Evaluating the toxicity profile of green-synthesized ferric nanoparticles using *madhuca indica* in a zebrafish model. *Biomed Mater Devices*, 1-15. <https://doi.org/10.1007/s44174-025-00348-8>
- [8] D. K. Sivaraj, S. S. Kumar, J. S. Dharmadhas, N. Al-Dayyan, S. Dhanasekaran, S. H. A. Aldhayan, et al. (2025) One-pot green synthesis and characterization of copper oxide nanoparticles with antibacterial and antioxidant properties using *Coleus amboinicus*. *Biomass Convers Biorefinery*, 15(15), 22429-22436. <https://doi.org/10.1007/s13399-023-04799-1>
- [9] A. Chauhan, J. Dhatwalia, V. Dutta, C. Gopalakrishnan, G. Rana, G.S. Hikku, et al.(2023) An investigation of the antimicrobial and antioxidant efficacy of copper oxide (I) nanoparticles: A green approach from *Myrica esculenta* fruit extract. *Chem Phys Impact*, 7, 100390. <https://doi.org/10.1016/j.chphi.2023.100390>
- [10] S.Ghotekar, C.R.Ravikumar, A.Chauhan, G.S. Hikku, K. Y. A., Lin, A. Rahdar, et al.(2024) Eco-friendly fabrication of CdO nanoparticles using *Polyalthia longifolia* leaves extract for antibacterial and electrochemical sensing studies. *JSGST*, 110 (1), 221-232. <https://doi.org/10.1007/s10971-024-06352-6>
- [11] S. A. Shilpa, C. Arthi, G. S. Hikku, K. Jeyasubramanian, P. Veluswamy, H. Ikeda (2024) Silver nanosphere/polycaprolactone coated cotton fabrics as hygienic textiles for health care industries. *Biointerface Res. App.*, 14(1), 1-19. <https://doi.org/10.33263/BRIAC141.011>
- [12] S. A. Shilpa, A. J. Pavithra, G. S. Hikku, K. Jeyasubramanian, P. Veluswamy, H. Ikeda (2023) Imparting efficient antibacterial activity to cotton fabrics by coating with green synthesized nano-Ag/PMMA composite. *BioNanoScience*, 13(4), 2180-2194. <https://doi.org/10.1007/s12668-023-01203-0>
- [13] A. Behera, K. R. Karthik, G. Shanmugam, U. S. Harshini, I. Rynthiang, D. S. Namrutha, et al.(2025) Antimicrobial activity of selenium

- nanoparticles–*Syzygium aromaticum* against oral pathogens. *Int Res J Multidiscip Technovation*. 7(6). <https://doi.org/10.54392/irjmt25617>
- [14] A. Sudha, J. Jeyakanthan, P. Srinivasan (2017) Green synthesis of silver nanoparticles using *Lippia nodiflora* aerial extract and evaluation of their antioxidant, antibacterial and cytotoxic effects. *RET*, 3(4), 506-515. <https://doi.org/10.1016/j.refit.2017.07.002>
- [15] N. Ostovar, N. Mohammadi, F. Khodadadeh (2023) Photocatalytic, antioxidant and antibacterial potential of bio-synthesized ZnO nanoparticles derived from espresso spent coffee grounds: optimization by central composite design. *Inorg Nano-Met Chem*, 53(9), 938-949. <https://doi.org/10.1080/24701556.2023.2187419>
- [16] C. N. Pope, D. Schlenk, F. J. Baud (2020) History and basic concepts of toxicology. In *An Introduction to Interdisciplinary Toxicology* (pp. 3-15). Academic Press. Elsevier. <https://doi.org/10.1016/B978-0-12-813602-7.00001-6>
- [17] D. J. Pohan, R. S. Marantuan, M. Djojaputro (2023) Toxicity test of strong drug using the BSLT (brine shrimp lethality test) method. *IJHSR*, 13(2), 203-209. <http://repository.uki.ac.id/id/eprint/10535>
- [18] C. Arulvasu, S. M. Jennifer, D. Prabhu, D. Chandhirasekar (2014) Toxicity effect of silver nanoparticles in brine shrimp *Artemia*. *Sci World J*, 2014(1), 256919. <https://doi.org/10.1155/2014/256919>
- [19] R. Tanino, Y. Amano, X. Tong, R. Sun, Y. Tsubata, M. Harada, et al. (2020) Anticancer activity of ZnO nanoparticles against human small-cell lung cancer in an orthotopic mouse model. *Mol Cancer Ther*, 19(2), 502-512. <https://doi.org/10.1158/1535-7163.MCT-19-0018>
- [20] P. Perumal, N. A. Sathakkathulla, K. Kumaran, R. Ravikumar, J. J. Selvaraj, V. Nagendran, et al. (2024) Green synthesis of zinc oxide nanoparticles using aqueous extract of shilajit and their anticancer activity against HeLa cells. *Sci Rep*, 14(1), 2204. <https://doi.org/10.1038/s41598-024-52217-x>
- [21] A. Hari Krishnan, B. Ramalingam, A. Nadeem, B. Ramachandran, V. K. Veena, S. Muthupandian (2024) Eco-friendly synthesis of zinc oxide nanoparticles (ZnO nps) from Piper betel leaf extract: spectral characterization and its application on plant growth parameters in maize, fenugreek and red gram. *Mater Technol*, 39(1), 2298547. <https://doi.org/10.1080/10667857.2023.2298547>
- [22] S. Rajeshkumar, S., Menon, S. V. Kumar, M. M. Tambuwala, H. A. Bakshi, M. Mehta, et al. (2019) Antibacterial and antioxidant potential of biosynthesized copper nanoparticles mediated through *Cissus arnotiana* plant extract. *Photochem Photobiol B: Biol*, 197, 111531. <https://doi.org/10.1016/j.jphotobiol.2019.111531>
- [23] R. Shanmugam, J. Anandan, A. K. Balasubramanian, R. D. Raja, S. Ranjeet, P. Deenadayalan, et al. (2023) Green synthesis of selenium, zinc oxide, and strontium nanoparticles and their antioxidant activity—a comparative in vitro study. *Cureus*, 15(12). DOI: 10.7759/cureus.50861
- [24] S. Fiddaroini, F. Prisilia, S. B. Karo, L. Madaniyah, A. D. Khairana, G. Rahmaniah, et al. (2025) Green synthesis of nanoparticles using cottonwood and rambutan honeys: Optimization, characterization, and enhanced antioxidant activity with reduced toxicity via oligochitosan coating. *Next Mater*, 8, 100685. <https://doi.org/10.1016/j.nxmater.2025.100685>
- [25] W. Tan, Y. Tian, Q. Zhang, S. Miao, W. Wu, X. Miao, et al. (2023) Antioxidant and antibacterial activity of *Apis laboriosa* honey against *Salmonella enterica* serovar Typhimurium. *Front Nutr*, 10, 1181492. <https://doi.org/10.3389/fnut.2023.1181492>
- [26] M. Chinnapaiyan, Y. Selvam, F. Bassyouni, M. Ramu, C. Sakkaraveeranan, A. Samickannian, et al. (2022) Nanotechnology, green synthesis and biological activity application of zinc oxide nanoparticles incorporated argemone mexicana leaf extract. *Molecules*, 27(5), 1545. <https://doi.org/10.3390/molecules27051545>
- [27] N. Assad, A. Abbas, M. F. ur Rehman, M. Naeem-ul-Hassan (2024) Photo-catalytic and biological applications of phyto-functionalized zinc oxide nanoparticles synthesized using a polar extract of *Equisetum diffusum* D. RSC adv, 14(31), 22344-22358. <https://doi.org/10.1039/D4RA03573A>
- [28] C. Aydin Acar, M. A. Gencer, S. Pehlivanoglu, S., Yesilot, S. Donmez (2024) Green and eco-friendly biosynthesis of zinc oxide nanoparticles using *Calendula officinalis* flower extract: Wound healing potential and antioxidant activity. *Int Wound J*, 21(1), e14413. <https://doi.org/10.1111/iwj.14413>
- [29] R. S. Dangana, R. C. George, F. K. Agboola (2023) The biosynthesis of zinc oxide nanoparticles using aqueous leaf extracts of *Cnidioscolus aconitifolius* and their biological activities. *Green Chem Lett Rev*, 16(1), 2169591. <https://doi.org/10.1080/17518253.2023.2169591>
- [30] P. Ramesh, A. Rajendran, M. Ashokkumar (2024) Biosynthesis of zinc oxide nanoparticles from *Phyllanthus Niruri* plant extract for photocatalytic and antioxidant activities. *Int J Environ Anal Chem*, 104(7), 1561-1572. <https://doi.org/10.1080/03067319.2022.2041004>
- [31] H. M. Berehu, S. Patnaik (2024) Biogenic zinc oxide nanoparticles synthesized from *Tinospora Cordifolia* induce oxidative stress, mitochondrial damage and apoptosis in colorectal cancer. *Nanotheranostics*, 8(3), 312. <https://doi.org/10.7150/ntno.84995>
- [32] Z. S. Amin, M. Afzal, J. Ahmad, N. Ahmed, B. Zeshan, N. H. H. N. Hashim, et al. (2023) Synthesis, characterization and biological activities of zinc oxide nanoparticles derived from secondary metabolites of *Lentinula edodes*. *Molecules*, 28(8), 3532. <https://www.mdpi.com/1420-3049/28/8/3532>
- [33] R. M. Varghese, A. Kumar, R. Shanmugam (2024) Antimicrobial activity of zinc oxide nanoparticles synthesized using *Ocimum tenuiflorum* and *Ocimum gratissimum* herbal formulation against oral pathogens. *Cureus*, 16(2). <https://doi.org/10.7759/cureus.53481>

IZVOD

BIOGENA SINTEZA NANOČESTICA CINK OKSIDA POMOĆU EKSTRAKTA *Coleus Amboinicus*: NJEGOVA SPEKTRALNA ANALIZA I BIOLOŠKE AKTIVNOSTI

Nanočestice cink oksida (ZnO NP) su sintetizovane korišćenjem ekstrakta lista *Coleus amboinicus* (CALE) putem zelenog sinteznog pristupa. UV-Vis spektroskopija je potvrdila formiranje ZnO NP, pokazujući široki pik na 335 nm. FTIR analiza je identifikovala fitohemikalije uključene u formiranje i pokrivanje ZnO NP, povećavajući stabilnost. SEM snimanje je otkrilo ZnO NP nepravilnog oblika veličine u rasponu od 20 nm do 50 nm, a EDAX je potvrdio elementarni sastav. ZnO NP sintetizovane korišćenjem CALE pokazale su snažnu antioksidativnu aktivnost u DPPH, H₂O₂, FRAP, ABTS i NO testovima. Visoka aktivnost, inhibicija zavisna od doze i sinergijski efekti ZnO NP i fitohemikalija ističu njihov potencijal za upotrebu u biomedicinskim i kozmetičkim primenama za ublažavanje oksidativnog stresa i upale. ZnO NP sintetizovane iz *C. amboinicus* pokazale su minimalnu citotoksičnost pri koncentracijama od 20 µg/mL u slanim škampima. U ćelijama osteosarkoma, ZnO NP su pokazale citotoksični efekat zavisan od doze sa IC₅₀ od 89,98 µg/mL. Morfološke promene i apoptoza ćelija osteosarkoma potvrđuju potencijal ZnO NP kao antikancerogenog sredstva.

Ključne reči: Cink oksid; nanočestice; antioksidativna aktivnost; toksikološka studija; antikancerogena aktivnost.

Naučni rad

Rad primljen: 18.12.2024.

Rad korigovan: 24.12.2025.

Rad prihvaćen: 07.01.2026.

Archana Behera:

<https://orcid.org/0009-0005-1448-9438>

Raeesha Rahman:

NA

Iadalin Ryntathiang:

<https://orcid.org/0009-0002-4341-1478>

Yuvashree Chandrasekaran:

<https://orcid.org/0000-0001-9673-4663>

Sridevi Kaliaperumal:

NA

Mukesh Kumar Dharmalingam Jothinathan:

<https://orcid.org/0009-0003-1161-346X>